



Research Article

Elastic–plastic solutions of reserved deformation for soft rock circular tunnel under high stress

Longyu Luo¹¹ College of Water Conservancy and Hydropower Engineering, Hohai University, Nanjing 210098, China

* Correspondence: 1262505774@qq.com

Received: 13 September 2024

Revised: 14 October 2024

Accepted: 15 October 2024

Published date: 16 October 2024

Doi: 10.70425/rml.202501.6



Copyright: © 2024 by the authors. This is an open-access article distributed under the terms of the Creative Commons Attribution License.

Abstract: The determination of reserved deformation is typically based on referring to relevant codes or the engineering analogy method, lacking a certain theoretical approach. The purpose of this study is to provide a theoretical basis for determining reserved deformation and to analyze the variation law of the surrounding rock affected by reserved deformation. Considering the reserved deformation under the condition of asymmetric load, the expression of optimal reserved deformation, the expression of support resistance reflecting the strength of surrounding rock, the strength of support material and the magnitude of in situ stress, the displacement expression of surrounding rock are derived by approximate solution based on the classical elastic–plastic theory. Numerical simulation software is used to simulate the displacement expression of the surrounding rock considering the reserved deformation and the expression of the optimum reserved deformation under the condition of asymmetric load. The results of the numerical simulation were compared with those of the analytical solutions, and the analytical results show that the errors between the two are within 12% and that the consistency is good.

Keywords: Reserved deformation; Circular cavity; Elasto-plastic solution

1. Introduction

In recent years, with the continuous development of geotechnical engineering towards deeper regions, more and more tunnels have experienced large deformation problems [1, 2]. Weak surrounding rock tunnel areas often show the characteristics of large deformation of initial support, strong rheology and poor self-stability of surrounding rock, complex tectonics and large tectonic stress [3]. To control the deformation of the soft rock tunnels, many scholars have proposed different support schemes [4–8]. Among them, setting reserved deformation is a commonly used support method in soft rock support systems. Setting a reserved deformation can control the displacement of the surrounding rock in a certain extent, the pressure of the surrounding rock can be released, and then reducing the support resistance [9]. In addition, considering the construction clearance of a tunnel, to a certain extent, the setting of reserved deformation can also ensure that there will be no intrusion of the support and that the clearance of the tunnel meets the design requirements. If the reserved deformation is too small and the deformation of the surrounding rock is greater than the reserved deformation, it will result in insufficient clearance of the tunnel. However, if the reserved deformation is too large, it will lead to the over-excavation of rock and increase construction costs. Therefore, during the construction of a soft rock tunnel, it is of great significance to study the excavation deformation law of surrounding rock, determine reasonable reserved deformation.

Actual engineering monitoring data can more accurately reflect the deformation characteristics of the surrounding rock [10]. By monitoring the displacement of the surrounding rock, the degree of damage to the surrounding rock, and the stress of the support structure, the monitoring data can be used to analyze and study the mechanism of the large deformation and failure of soft rock [11, 12]. Laboratory model testing is a common method for studying the large deformation of soft rock [13, 14]. Through model experiments, the creep deformation and failure characteristics of soft rock tunnels under combined support conditions can be analysed [15]. Different conditions can also be set to analyse the deformation and stress changes of tunnels under different geological conditions [16]. It is possible to analyse the control effects of different support measures on large deformation of surrounding rock [15, 17, 18] and analyse relevant influencing factors [19]. With the rapid development of computer technology, many numerical simulation calculation software programs have emerged, such as FLAC 3D [20, 21], ANAYS [22, 23], and ABQUES [24, 25]. Therefore, scholars also use numerical simulation software to analyse the laws of the large deformation of soft rock. However,

the construction of a theoretical model is the theoretical basis for analysing the deformation and failure mechanisms of the surrounding rock. Scholars have also used theoretical modelling methods to study the deformation mechanism of soft rock. There are many existing models for analysing the large deformation of soft rock [26]. These include an elastic–plastic constitutive model of soft rock with strain softening [27], Alejano and Alonso’s model [28], Walton et al.’s model [29] and Rahjoo and Eberhardt’s model [30]. By establishing a mechanical model of the tunnel excavation-support process, an analytical solution can be obtained between the stress and displacement of the surrounding rock [31], and the contact friction slip contact problem between the surrounding rock and the lining can be analysed [32]. Based on the above research status, it can be concluded that scholars mainly analyse the failure mechanism of large deformation of soft rock through laboratory and field tests, on-site monitoring, numerical simulation and the establishment of relevant constitutive models.

However, the research of reserved deformation only focuses on providing a range of values for reserved deformation under different working conditions for different projects. Ma Zhaolin and Wang Yue [33] relied on the data of Gu-chengling tunnel of Baoji-Lanzhou Railway Line for passenger traffic and used FLAC 3D software to predict the deformation of the initial support structure and optimized the design reserve deformation of the tunnel. Yang Wenhui [34] conducted a comprehensive evaluation of the deformation of the surrounding rock of Jiufengshan Tunnel through data statistics, and determined the reasonable range of reserved deformation for Jiufengshan Tunnel. Yu Weigang [35] et al. studied the reserved deformation of the Baima Tunnel by using probability and statistical methods under different support parameters. Liu Jian [36] et al. analyzed 148 monitoring section data of tunnels with different types of loess soil, and obtained recommended values for the reasonable design of reserved deformation in loess tunnels. So at present, the reserved deformation is mainly determined based on engineering analogy, reference to relevant standards and numerical simulation methods. However, different designers may have certain deviations in determining the reserved deformation due to their different work experiences, and this method does not have a theoretical basis. At present, classical elastic–plastic theory is often applied to analyse the deformation and failure laws of surrounding rock in caverns [31]. There is no established theoretical expression of the relationship between reserved deformation and the support system. Therefore, this article aims to derive an expression for the reserved deformation from the perspective of analytical solutions, to

provide a theoretical basis for determining the reserved deformation. According to the expression of the reserved deformation, the corresponding reserved deformation can be obtained by substituting the relevant surrounding rock parameters, crustal stress conditions, and support strength parameters. Through equation substitution, the expression of the variation of the surrounding rock displacement with the reserved deformation can be obtained. Thus, the impact of the reserved deformation on the displacement of the surrounding rock can be analysed.

In response to the problems mentioned above, according to classical elastic-plastic theory, this article uses approximate solutions to transform the plane problem of surrounding rock under non-axisymmetric conditions into a plane problem under axisymmetric conditions. Therefore, the displacement expression of the surrounding rock considering reserved deformation under non-axisymmetric conditions, the expression of reserved deformation, and the expression of support resistance are solved. To have a clearer understanding of which influencing factors affect the reserved deformation, an analysis of the influencing factors was conducted on the expression of the reserved deformation. Subsequently, based on numerical simulation experiments, the variation laws and errors between the numerical and analytical solutions of the reserved deformation expression and the displacement expressions of surrounding rock considering reserved deformation were compared and analysed. The purpose of this study is to provide a theoretical basis for determining reserved deformation and to analyse the variation law of the surrounding rock affected by reserved deformation.

2. Elasto-plastic solution of circular cavity under non-axisymmetric conditions

When the rock is excavated, the initial stress state is destroyed and resulting in stress adjustments [37]. In a certain area of the tunnel wall, the adjusted stress generally exceeds the elastic limit of the rock mass. At this point, the rock mass near the tunnel wall will enter a plastic state, while the rock mass far away from the tunnel wall will gradually transition to an elastic state, as shown in Figure 1 [38].

In the construction process of soft rock tunnels, reserved deformation is a special support method. The size of the reserved deformation determines the excavation radius and stress adjustment range of the tunnel. However, many classic analytical solutions do not involve the problem of reserved deformation. Therefore, based on the elastic-plastic solution derived by predecessors for circular cavities, this article derives the relevant analytical solution for circular cavities considering the reserved deformation.

However, in construction, the geological conditions of the surrounding rock are complex and variable. When conducting theoretical analysis and research, it is necessary to simplify the surrounding rock conditions. If the spacing between structural planes or joints in the rock mass is relatively wide, structural planes or joints are tightly closed, and the stress value of the surrounding rock is less than half of the compressive strength of the rock mass, the surrounding rock can be approximately judged as an elastic rock mass [39]. so the following assumptions are made:

- (1) The surrounding rock is homogeneous, isotropic and continuous.
- (2) The influence of gravitational acceleration is neglected under sufficiently large burial depth conditions.
- (3) Since the tunnel is long enough, the plane problem of the tunnel can be considered a plane strain problem.

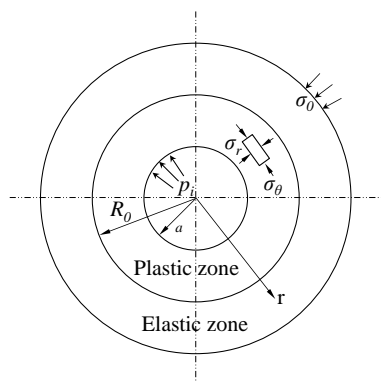


Fig. 1. Sketch of tunnel mechanical analysis model

2.1. General and approximate solutions under non-axisymmetric conditions

In practical engineering, the loads on tunnels are often non-axisymmetric. Therefore, for circular cross-section tunnels, under non-axisymmetric load conditions, the stress and deformation at a point in the surrounding rock are related to the position, so the stress and displacement at that point are functions of *r* and *θ*. Then the equilibrium differential equation is as follows

$$\begin{cases} \frac{\partial \sigma_r}{\partial r} + \frac{1}{r} \frac{\partial \tau_{r\theta}}{\partial \theta} + \frac{\sigma_r - \sigma_\theta}{r} = 0 \\ \frac{1}{r} \frac{\partial \sigma_\theta}{\partial \theta} + \frac{\partial \tau_{r\theta}}{\partial r} + \frac{2\tau_{r\theta}}{r} = 0 \end{cases} \quad (1)$$

According to the molar strength criterion, the yield conditions that the surrounding rock needs to meet are as follows

$$4\tau_{r\theta}^2 = (\sigma_\theta \sin \varphi + \sigma_r \sin \varphi + 2C \cos \varphi)^2 - (\sigma_\theta - \sigma_r)^2 \quad (2)$$

where σ_r, σ_θ, τ_{rθ} is an unknown quantity.

According to the relevant boundary conditions, it should be possible to calculate the stress component of the plastic zone, but the solution is more difficult. When the tunnel is under non-axisymmetric load conditions, an elliptical plastic zone will appear in the surrounding rock and the surrounding strata in the plastic zone will gradually become uniform. At this time, the unequal pressure of the original rock stress can be converted according to equation (3) [40]. Through the equivalent transformation of stress in equation (3), the tunnel problem under non-axisymmetric load conditions can be simplified as an axisymmetric problem under hydrostatic pressure and plane strain conditions

$$\sigma_0 = \frac{1 + \lambda}{2} P_v \quad (3)$$

where σ₀ is the equivalent stress; λ is the ratio of horizontal stress and vertical stress of surrounding rock, i.e. the lateral coefficient of earth pressure; and P_v is the vertical stress. Therefore, this article simplifies the non-axisymmetric load condition to an axisymmetric load condition based on equation (3) and conducts a relevant solution analysis based on the solution ideas under axisymmetric conditions.

2.2. Solution of relevant expressions under non-axisymmetric conditions

In classical elastic-plastic theory, the expression for the stress field in the plastic zone is

$$\begin{cases} \sigma_r^p = (p_i + C \cot \varphi) \left(\frac{r}{a} \right)^{\frac{2 \sin \varphi}{1 - \sin \varphi}} - C \cot \varphi \\ \sigma_\theta^p = (p_i + C \cot \varphi) \left(\frac{1 + \sin \varphi}{1 - \sin \varphi} \right) \left(\frac{r}{a} \right)^{\frac{2 \sin \varphi}{1 - \sin \varphi}} - C \cot \varphi \end{cases} \quad (4)$$

The stress field of the surrounding rock in the elastic zone is as follows

$$\begin{cases} \sigma_r^e = \sigma_0 \left(1 - \frac{R_0^2}{r^2} \right) + \sigma_{R_0} \frac{R_0^2}{r^2} \\ \sigma_\theta^e = \sigma_0 \left(1 + \frac{R_0^2}{r^2} \right) - \sigma_{R_0} \frac{R_0^2}{r^2} \end{cases} \quad (5)$$

Due to the condition that the stress on the boundary of the elastic and plastic regions is equal, the following can be obtained

$$\sigma_r^p + \sigma_\theta^p = \sigma_r^e + \sigma_\theta^e = 2\sigma_0 \quad (6)$$

Bringing the stress component of the plastic zone, i.e. equation (4), into equation (6), equation (7) can be solved as follows

$$R_0 = a \left[\frac{(\sigma_0 + C \cot \varphi)(1 - \sin \varphi)}{p_i + C \cot \varphi} \right]^{\frac{1 - \sin \varphi}{2 \sin \varphi}} \quad (7)$$

Equation (7) represents the radius of the plastic zone under an axisymmetric loading condition. Referring to the approximate solution method of equation (3), bringing σ₀=[(1+λ)/2]P_v into equation (7) can obtain the plastic zone radius under non-axisymmetric conditions as follows

$$R_0 = a \left[\frac{\left(\frac{1 + \lambda}{2} P_v + C \cot \varphi \right) (1 - \sin \varphi)}{p_i + C \cot \varphi} \right]^{\frac{1 - \sin \varphi}{2 \sin \varphi}} \quad (8)$$

Transforming equation (8) into an equation, the support resistance p_i can be solved as follows

$$p_i = \left(\frac{1 + \lambda}{2} P_v + C \cot \varphi \right) (1 - \sin \varphi) \left(\frac{a}{R_0} \right)^{\frac{2 \sin \varphi}{1 - \sin \varphi}} - C \cot \varphi \quad (9)$$

Equation (9) is the famous modified Finner formula. It can be seen from equation (9) that under the condition of a non-axisymmetric load, the support resistance p_i is related to vertical pressure P_v , lateral pressure coefficient λ , plastic zone radius R_0 , cohesive force C of surrounding rock in the plastic zone, internal friction angle φ , and tunnel radius a .

In the stage of elastic-plastic deformation, the stress and strain are nonlinear in the plastic zone, so the constitutive equation of the surrounding rock cannot be expressed by the generalized Hooke's law. The common method for calculating the displacement expression is to use the relationship between the average stress σ_m and the average strain ε_m , multiply that by the plastic modulus ψ , and assume that the volumetric strain in the plastic zone is zero; the displacement of the surrounding rock in the plastic zone can be obtained [41]. In equation (10), Genka proposed using $G' = G/\psi$ instead of G to obtain the elastic-plastic constitutive relationship, abbreviated as the Genka equation [42] as follows

$$\begin{cases} \varepsilon_r = \frac{\psi}{2G} (\sigma_r - \sigma_m), & \gamma_{r\theta} = \frac{\psi}{G} \tau_{r\theta} \\ \varepsilon_\theta = \frac{\psi}{2G} (\sigma_\theta - \sigma_m), & \gamma_{\theta z} = \frac{\psi}{G} \tau_{\theta z} \\ \varepsilon_z = \frac{\psi}{2G} (\sigma_z - \sigma_m), & \gamma_{zr} = \frac{\psi}{G} \tau_{zr} \end{cases} \quad (10)$$

where ψ is the plastic modulus representing the nonlinear relationship between average stress and average strain. The problem of a section of a tunnel is simplified to a plane strain problem in the analysis, so $\varepsilon_z = \gamma_{\theta z} = \gamma_{z\theta} = 0$, then there are:

$$\sigma_m = (\sigma_r + \sigma_\theta) / 2 \quad (11)$$

The elastic-plastic constitutive relation under plane strain problem can be obtained by substituting equation (12) into equation (11) as follows

$$\begin{cases} \varepsilon_r = \frac{\psi}{4G} (\sigma_r - \sigma_\theta) \\ \varepsilon_\theta = \frac{\psi}{4G} (\sigma_\theta - \sigma_r) \\ \gamma_{r\theta} = \frac{\psi}{G} \tau_{r\theta} \end{cases} \quad (12)$$

On the boundary of the elastic and plastic zones, there is $\psi = 1$. By solving geometric equations under axisymmetric loading conditions, equation (13) can be obtained as follows

$$\varepsilon_\theta = A r^{-2} \quad (13)$$

where A is the integration constant. After substituting equation (13) into equation (12), and then bringing in equation (4), equation (13) can be obtained as follows

$$A = \frac{R_0^2}{4G} (p_i + C \cot \varphi) \left(\frac{2 \sin \varphi}{1 - \sin \varphi} \right) \left(\frac{R_0}{a} \right)^{\frac{2 \sin \varphi}{1 - \sin \varphi}} \quad (14)$$

Substituting the modified Finner equation (9) into equation (14), we have

$$A = \frac{R_0^2}{2G} (\sigma_0 + C \cot \varphi) \sin \varphi \quad (15)$$

Bringing equation (15) into equation (13) and then into the geometric equation $\varepsilon_\theta = \mu/r$, the expression of calculating elastic-plastic displacement of the circular tunnel under axisymmetric conditions can be obtained as follows

$$u^p = r \varepsilon_\theta = \frac{A}{r} = \frac{R_0^2}{2Gr} (\sigma_0 \sin \varphi + C \cot \varphi) \quad (16)$$

Substituting $\sigma_0 = [(1 + \lambda)/2] P_v$ into equation (16), the expression of elastic-plastic displacement of the circular tunnel under asymmetric conditions can be obtained as follows

$$u^p = \frac{R_0^2}{2Gr} \left(\frac{1 + \lambda}{2} P_v \sin \varphi + C \cot \varphi \right) \quad (17)$$

Equation (17) shows that displacement u^p of plastic zone of the surrounding rock is related to radius R_0 of plastic zone, the mechanical

parameter C , φ and G of the surrounding rock, lateral pressure coefficient λ and vertical pressure P_v .

In this section, the relevant expressions for the plane problem of the surrounding rock under non-axisymmetric conditions are derived by the approximate solution method. Based on the expressions derived above, the derivation of the elastic-plastic solution of the circular cavity considering the reserved deformation can be further carried out.

3. Elasto-plastic solution of circular cavity considering reserved deformation

Setting reserved deformation is a commonly used support method in soft rock support systems. Setting appropriate reserved deformation can release a certain degree of surrounding rock pressure, control the displacement of surrounding rock, reduce support resistance, and improve the safety reserve of the secondary lining [9]. During the construction of soft rock tunnels, it is of great significance to study the excavation deformation law of surrounding rock, determine reasonable reserved deformation, and guarantee the stability of tunnel chambers. Therefore, based on the simplified expressions under non-axisymmetric load conditions, the following section will solve the elastic-plastic expression for circular cavities, considering the reserved deformation.

3.1. Solution of displacement expression for surrounding rock

Before deriving the expression, it is necessary to have a clear understanding of the reserved deformation. We all know that the support system of thnnel gennely include the initial suppot and the secondary lining. In order to prevent the large deformation of surrounding rock, a space usually is reserved between the initial support and the secondary lining. The space usually call reserved deformation, as shown in Figure 2.

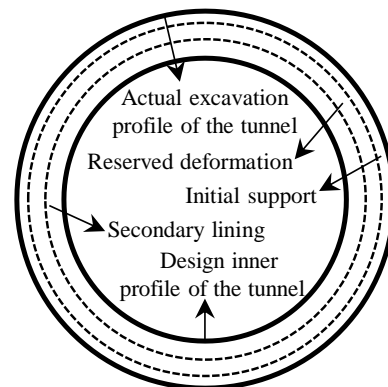


Fig. 2. Schematic diagram of expected deformation in a soft rock support system

If the reserved deformation is set between the initial support and the secondary lining, the clearance of the tunnel section will be reduced. To meet the construction clearance requirements of the tunnel, the original excavation section of the tunnel design needs to be expanded, which is equal to the designed reserved deformation. In the large deformation support system of soft rock, if the reserved deformation is set as m , the excavation radius of the tunnel changes from a to $m+a$, so the expression of plastic radius, i.e. equation (8), can be rewritten as follows

$$R_0 = (m + a) \left[\frac{\left(\frac{1 + \lambda}{2} P_v + C \cot \varphi \right) (1 - \sin \varphi)}{P_i + C \cot \varphi} \right]^{\frac{1 - \sin \varphi}{\sin \varphi}} \quad (18)$$

Substituting equation (18) into the expression of displacement of plastic zone under asymmetric load, i.e. equation (17), the displacement of plastic zone can be obtained as follows:

$$u^p = \frac{(m + a)}{2Gr} \sin \varphi \left(\frac{1 + \lambda}{2} P_v + C \cot \varphi \right) \times \left[\frac{\left(\frac{1 + \lambda}{2} P_v + C \cot \varphi \right) (1 - \sin \varphi)}{P_i + C \cot \varphi} \right]^{\frac{1 - \sin \varphi}{\sin \varphi}} \quad (19)$$

There is $r = m + a$ at the tunnel wall, so the displacement at the tunnel wall is as follows

$$u_0 = \frac{(m + a) \left(\frac{1 + \lambda}{2} P_v + C \cot \varphi \right) \sin \varphi}{2G} \times \left[\frac{\left(\frac{1 + \lambda}{2} P_v + C \cot \varphi \right) (1 - \sin \varphi)}{P_i + C \cot \varphi} \right]^{\frac{1 - \sin \varphi}{\sin \varphi}} \quad (20)$$

From equation (20), it can be seen that the displacement u_0 of surrounding rock is determined by the in vertical stress P_v , support resistance p_i , lateral pressure coefficient λ , original radius a of the tunnel and the reserved deformation m , support resistance p_i , mechanical parameters C, φ and G of the surrounding rock.

When the support resistance p_i is a fixed value, the trend of displacement u_0 of surrounding rock at the tunnel wall along with the reserved deformation m is plotted, as shown in Figure 3.

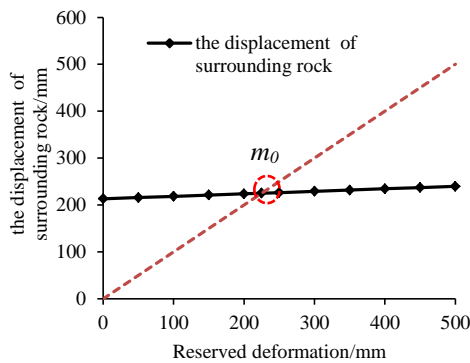


Fig. 3. Trend diagram of surrounding rock displacement with reserved deformation

The dotted red line in Figure 3 is the angular bisector, and the points on the angular bisector indicate that the displacement u_0 of surrounding rock and the reserved deformation m are equal. It can be seen that with the increase of reserved deformation m , the displacement u_0 of surrounding rock will gradually increase. If the displacement u_0 of surrounding rock is above the angular bisector, u_0 is greater than m , indicating that the tunnel has an intrusion limit. If u_0 is below the angular bisector, it is less than m , indicating that the tunnel is over-excavated. If u_0 is located on the angular bisector, i.e. at the intersection point m_0 of the solid line and the dashed line, then u_0 equals m , indicating that there is neither over-excavation nor intrusion in the tunnel.

3.2. Solution for optimal reserved deformation

The purpose of setting the reserved deformation m is to prevent the surrounding rock from intruding into the design contour and to reduce the project costs. The results of Figure 3 show that when $u_0 = m_0$, neither intrusion nor over-excavation occurs in the tunnel. Therefore, under the action of support resistance p_i , when the displacement u_0 of surrounding rock just reaches the optimum reserved deformation m_0 , the surrounding rock is stable and no displacement occurs. At this time, it is considered that the reserved deformation is the most reasonable. Therefore, ideally, the following assumptions can be made.

(1) The displacement of the surrounding rock does not occur after reaching the optimal reserved deformation m_0 , and the surrounding rock is stable.

(2) The value of support resistance p_i is a fixed value and does not change with the change of the surrounding rock stress field.

Based on the above assumptions, it can be inferred that if the optimal reserved deformation m_0 was set, the tunnel radius will change from a to $a + m$. After the tunnel was supported, the maximum displacement of the surrounding rock is reserved deformation, and it can be obtained that:

$$u_0 = m_0 \quad (21)$$

By substituting equation (21) into the expression (20) for the displacement u_0 of surrounding rock, it can be obtained that

$$m_0 = \frac{(m_0 + a) \left(\frac{1 + \lambda}{2} P_v + C \cot \varphi \right) \sin \varphi}{2G} \times \left[\frac{\left(\frac{1 + \lambda}{2} P_v + C \cot \varphi \right) (1 - \sin \varphi)}{P_i + C \cot \varphi} \right]^{\frac{1 - \sin \varphi}{\sin \varphi}} \quad (22)$$

According to the basic properties of the equation, the optimum reserved deformation m_0 can be solved using equation (22) as follows

$$m_0 = \frac{\left(\frac{1 + \lambda}{2} P_v + C \cot \varphi \right) a \sin \varphi}{2G - \left(\frac{1 + \lambda}{2} P_v + C \cot \varphi \right) \sin \varphi} \times \left[\frac{\left(\frac{1 + \lambda}{2} P_v + C \cot \varphi \right) (1 - \sin \varphi)}{P_i + C \cot \varphi} \right]^{\frac{1 - \sin \varphi}{\sin \varphi}} \times \left[\frac{\left(\frac{1 + \lambda}{2} P_v + C \cot \varphi \right) (1 - \sin \varphi)}{P_i + C \cot \varphi} \right]^{\frac{1 - \sin \varphi}{\sin \varphi}} \quad (23)$$

Assume that

$$\begin{cases} \alpha = \frac{1 + \lambda}{2} P_v + C \cot \varphi \\ \beta = 1 - \sin \varphi \end{cases} \quad (24)$$

Then equation (24) can be simplified to

$$m_0 = \frac{\alpha \sin \varphi \left(\frac{\alpha \beta}{P_i + C \cot \varphi} \right)^{\frac{\alpha}{\sin \varphi}}}{2G - \alpha \sin \varphi \left(\frac{\alpha \beta}{P_i + C \cot \varphi} \right)^{\frac{\alpha}{\sin \varphi}}} a \quad (25)$$

Equation (25) is the expression of the optimal reserved deformation m_0 of the surrounding rock in an elastic-plastic state. From equation (25), it can be seen that the optimum reserved deformation m_0 is related to the in situ stress P_v , support resistance p_i , lateral pressure coefficient λ , original radius a of tunnel, and mechanical parameters C, φ, G of surrounding rock.

3.3. Solution to support resistance

In the design stage of the tunnel, the support resistance p_i is unknown, so it is necessary to determine the reserved deformation m_0 in advance to design the relevant support structure. If the displacement of the surrounding rock at the tunnel wall is equal to the reserved displacement m_0 , then there is $u_0 = m_0$. Substituting $u_0 = m_0$ into equation (17), there is:

$$m_0 = \frac{R_0^2}{2G(m_0 + a)} \left(\frac{1 + \lambda}{2} P_v \sin \varphi + C \cot \varphi \right) \quad (26)$$

According to equation (26), radius R_0 of plastic zone can be solved as follows

$$R_0 = \left[\frac{2m_0 G(m_0 + a)}{\frac{1 + \lambda}{2} P_v \sin \varphi + C \cot \varphi} \right]^{\frac{1}{2}} \quad (27)$$

Substituting equation (27) into equation (9), the support resistance p_i can be solved as follows

$$p_i = \left(\frac{1 + \lambda}{2} P_v + C \cot \varphi \right) (1 - \sin \varphi) \times \left[\frac{\left(\frac{1 + \lambda}{2} P_v \sin \varphi + C \cot \varphi \right) (m_0 + a)}{2m_0 G} \right]^{\frac{\sin \varphi}{1 - \sin \varphi}} - C \cot \varphi \quad (28)$$

Substituting equation (24) into equation (28), equation (28) can be simplified as follows

$$p_i = \alpha \beta \left[\frac{\alpha(m_0 + a) \sin \varphi}{2m_0 G} \right]^{\frac{\sin \varphi}{\beta}} - C \cot \varphi \quad (29)$$

Since $G = E/[2 \times (1 + \mu)]$, equation (29) can be changed to

$$p_i = \alpha \beta \left[\frac{\alpha(1 + \mu)(m_0 + a) \sin \varphi}{m_0 E} \right]^{\frac{\sin \varphi}{\beta}} - C \cot \varphi \quad (30)$$

In practical engineering, the radial displacement u of the tunnel wall mainly consists of two parts: the radial displacement u_1 from the excavation of the tunnel to the setting of the support and the radial

displacement u_2 after the setting of the support. Due to the assumption that the reserved deformation is equal to the displacement of the surrounding rock

$$m_0 = u = u_1 + u_2 \tag{31}$$

At present, the measured relationship curve between the displacement of the tunnel wall and excavation time t under unknown protection is generally used to calculate u_1 . For the circular section tunnel with a closed concrete lining, according to the assumption of the joint deformation of the surrounding rock and support, the expression of u_2 related to the form of the support structure can be solved according to the thick-walled tube theory of elasticity.

Under axisymmetric load conditions, it is assumed that there is a cylinder with an inner diameter of r and an outer diameter of R , which is affected by internal pressure q_1 and external pressure q_2 . According to the relevant theory of a thick-walled cylinder, the stress component of the cylinder under uniformly distributed pressure can be obtained, which is the Lamé solution.

$$\begin{cases} \sigma_\rho = \frac{R^2}{\rho^2} - 1 & 1 - \frac{r^2}{\rho^2} \\ \sigma_\varphi = \frac{R^2}{\rho^2} + 1 & 1 + \frac{r^2}{\rho^2} \end{cases} \begin{cases} q_1 - \frac{r^2}{R^2} q_2 \\ q_1 - \frac{r^2}{R^2} q_2 \end{cases} \tag{32}$$

According to assumption (2) in section 3.2, the initial support is equivalent to a thick-walled cylinder subjected to an axisymmetric external pressure P_i , and then there is

$$\begin{cases} q_1 = 0 \\ q_2 = P_i \end{cases} \tag{33}$$

Substituting equation (32) into equation (33), it can be obtained that

$$\begin{cases} \sigma_\rho = -\frac{1 - \frac{r^2}{\rho^2}}{1 - \frac{R^2}{R^2}} P_i \\ \sigma_\varphi = -\frac{1 + \frac{r^2}{\rho^2}}{1 - \frac{R^2}{R^2}} P_i \end{cases} \tag{34}$$

The corresponding expressions of the radial surrounding rock displacement under external pressure p_i can be obtained as follows

$$u_\rho = -\frac{P_i}{E} \left[\frac{(1 + \mu) + \frac{\rho^2(1 - \mu)}{r^2}}{\rho \left(\frac{1}{r^2} - \frac{1}{R^2} \right)} \right] \tag{35}$$

When $\rho=R$, the displacement u_2 at the outer diameter of the lining can be obtained as follows

$$u_2 = -\frac{P_i R}{E'} \left[\frac{r^2 + R^2}{r^2 - R^2} - \mu' \right] \tag{36}$$

where r is the inner radius of the support, R is the external radius of support, E' and μ' are elastic modulus and Poisson ratio of the support materials. Substituting equation (36) into equation (31), equation (37) can be obtained as follows

$$m_0 = u = u_1 + \frac{P_i R}{E'} \left(\frac{r^2 + R^2}{r^2 - R^2} - \mu' \right) \tag{37}$$

Substituting equation (37) into equation (30), equation (38) can be obtained as follows

$$P_i = \alpha\beta \left\{ \frac{\alpha(1 + \mu) \left[u_1 + \frac{P_i R}{E'} \left(\frac{r^2 + R^2}{r^2 - R^2} - \mu' \right) + a \right] \sin \varphi}{\left[u_1 + \frac{P_i R}{E'} \left(\frac{r^2 + R^2}{r^2 - R^2} - \mu' \right) \right] E} \right\}^{\frac{\sin \varphi}{\beta}} - C \cos \varphi \tag{38}$$

From equation (38), it can be seen that the support resistance p_i is related to the strength parameters C , φ , E of surrounding rock, structural

and strength parameters r , R , E' , μ' of support materials, vertical stress P_v , lateral pressure coefficient λ and tunnel radius a .

Similarly, when $\rho=R$ and the lining is in the critical state of failure, the stress reaches the compressive strength σ_c . According to equation (34), it can be concluded that the stress at the outer diameter of the lining needs to be satisfied:

$$P_i \leq \frac{R^2 - r^2}{R^2 + r^2} \sigma_c \tag{39}$$

Based on equations (38) and (39), the support structure can be designed in the limit state.

4. Analysis of influencing factors of optimal reserved deformation

Analysing the influencing factors of an expression can better explain the law of the variable being influenced by other variables [43–45]. From equation (25), it can be seen that the optimum reserved deformation m_0 is related to in situ stress P_v , support resistance p_i , lateral pressure coefficient λ , tunnel radius a , and mechanical parameters C , φ , E , μ of surrounding rock. To study the variation laws of the optimal reserved deformation influenced by these variables, this article conduct a quantitative analysis of these influencing factors. The basic parameters of the surrounding rock are shown in Table 1. The influence of a single factor on the optimal reserved deformation m_0 is analysed by changing its value.

Due to the grade of the surrounding rock with large deformation is usually not high, the values of influencing factors are selected according to the relevant codes where list the physical and mechanical property indicators of different surrounding rock grades and own experience. The values of each influencing factor are as follows: (a) The values of vertical stress P_v are 0 MPa, 5 MPa, 10 MPa, 15 MPa, 20 MPa, 25 MPa and 30 MPa; (b) The values of support resistance p_i are 0.5 MPa, 1 MPa, 2 MPa, 3 MPa, 4 MPa, 5 MPa and 6 MPa; (c) The values of modulus of elasticity G are 1 GPa, 2 GPa, 3 GPa, 4 GPa, 5 GPa, 6 GPa and 7 GPa; (d) The tunnel radius of a are 1 m, 2 m, 3 m, 4 m, 5 m, 6 m, 7 m; (e) The values of internal friction angle φ are 31°, 32°, 33°, 34°, 35°, 36° and 37°; (f) The values of cohesion C are 0.1 MPa, 0.2 MPa, 0.3 MPa, 0.4 MPa, 0.5 MPa, 0.6 MPa and 0.7 MPa.

Refer to Table 1 for the values of other relevant parameters. At different lateral pressure coefficient λ , the trend curve of the optimal reserved deformation m_0 with different influencing factors is plotted as shown in Figure 4. It can be seen from Figure 4(a) that at different lateral pressure coefficients λ , the optimal reserved deformation m_0 gradually increases with the increase of vertical pressure P_v . The curves show an upward trend of concave curves, which indicates that the variation of the optimal reserved deformation m_0 gradually increases. At the same vertical pressure P_v , the larger the lateral pressure coefficient λ is, the larger the required optimal reserved deformation m_0 is.

As shown in Figure 4(b), with the increase of support resistance p_i , the optimum reserved deformation m_0 will gradually decrease and the amplitude of change will gradually decrease. At the same support resistance p_i , the larger the lateral pressure coefficient λ is, the larger the required optimal reserved deformation m_0 is.

From Figure 4(c), it can be seen that the change trend of the optimal reserved deformation m_0 with the modulus of elasticity E is the same as the change trend with the support resistance p_i . Under different lateral pressure coefficients λ , the optimal reserved deformation m_0 gradually decreases with the increase of modulus of elasticity E , and the amplitude of change gradually decreases. At the same modulus E , the larger the lateral pressure coefficient λ is, the larger the optimal reserved deformation m_0 is.

From Figure 4(d), it can be seen that the curve shows a linear increase with the increase in radius a . This indicates that the optimal reserved deformation m_0 will gradually increase with a constant change. At the same tunnel radius a , the larger the lateral pressure coefficient λ is, the larger the required optimal reserved deformation m_0 is. With increases of λ , the slope of the line becomes larger, indicating a larger variation in the optimal reserved deformation.

It can be seen from Figure 4(e) that at different lateral pressure coefficients λ , the curve shows a decreasing trend of the concave curve with the increase of the internal friction angle φ , which means that the optimal reserved deformation m_0 will gradually decrease. At the same internal friction angle φ , the larger the λ is, the larger the required optimal reserved deformation m_0 is.

From Figure 4(f), it can be seen that the trend of the optimal reserved deformation m_0 with cohesion C is the same as the trend of the optimal reserved deformation m_0 with internal friction angle φ . At different lateral

pressure coefficients λ , the optimal reserved deformation m_0 gradually decreases with the increase of cohesion C , and the curve shows a downward trend of concave curve, indicating that the reduction of the

optimal reserved deformation is gradually decreasing. At the same cohesion C , the larger the lateral pressure coefficient λ , the larger the required optimal reserved deformation m_0 is.

Table 1. Basic parameters of surrounding rock under influence factor analysis

Tunnel radius a/m	Elastic modulus E/GPa	Vertical pressure P_v/MPa	Cohesion C/MPa	Internal friction angle $\phi/^\circ$	Poisson ratio μ	Lateral pressure coefficient λ	Support resistance p_i/MPa
4	2	20	0.1	35	0.35	0.5、0.75、1、1.25、1.5	1

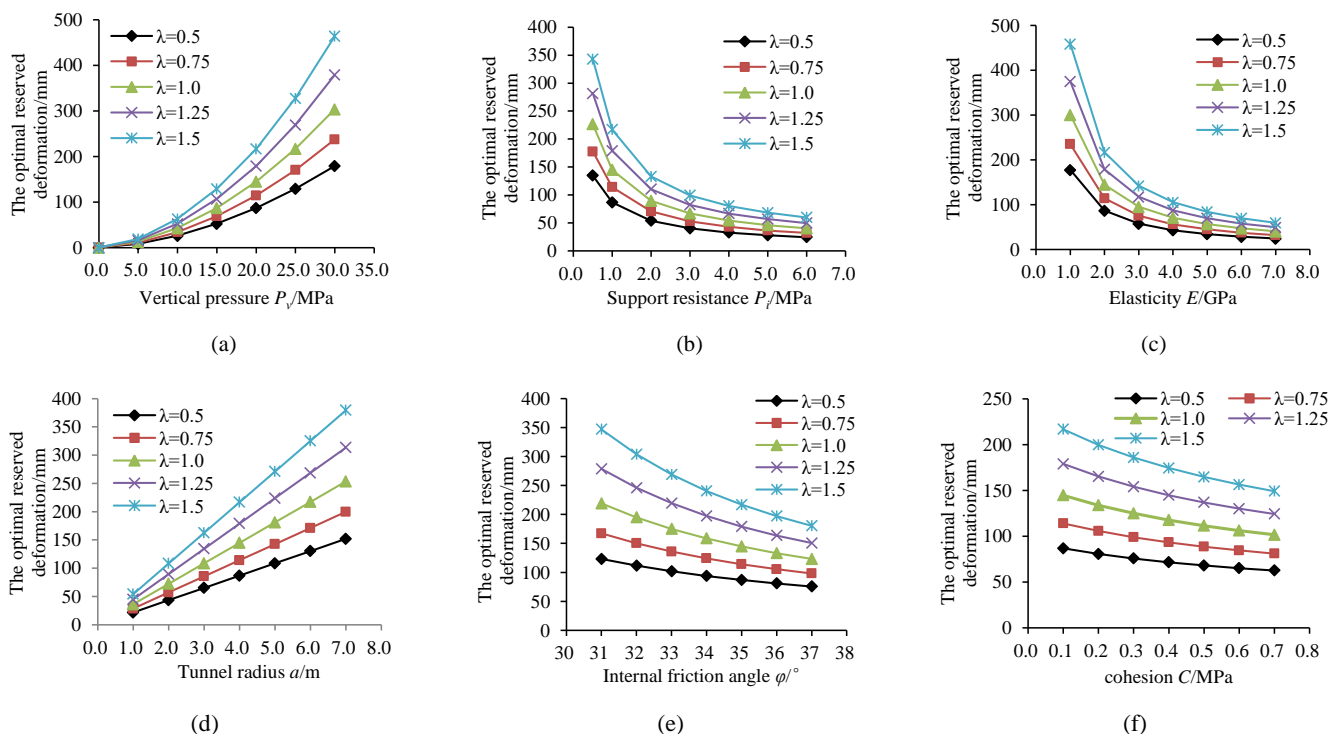


Fig. 4. The trend curve of the optimal reserved deformation amount with different influencing factors

5. Comparison analysis of numerical solution and analytical solution considering the reserved deformation

FLAC 3D is a numerical simulation software for geotechnical engineering. With the continuous improvement of FLAC 3D, many scholars have chosen FALC 3D software to conduct relevant analyses and research on rock engineering [46–49]. In this paper, FLAC 3D is used to simulate the displacement of surrounding rock considering the reserved deformation, and compare it with result of equation (20). Simultaneously FLAC 3D was used to determine the optimal reserved deformation and compare it with the result of equation (23).

5.1. Comparative analysis of numerical and analytical solutions for the expression equation of surrounding rock displacement

During the numerical simulation, the support resistance and the reserved deformation m must be determined firstly, then compare the error of surrounding rock displacement with the change of reserved deformation m under the two methods of analytical solution and numerical simulation.

The modelling method for numerical models refers to Yang and Gao's [50] modelling method. The model size is $88 \times 88 \times 1m$, and the values of the reserved deformation m are taken as 0, 10, 20, 30, 40 and 50mm in sequence. Since equation (20) is derived based on elastic–plastic theory, the Mohr Coulomb model is selected as the constitutive model. According to the Saint-Venant principle [49], the surrounding rock outside the range of five times the tunnel diameter is not affected by the tunnel excavation, so the left, right, front, rear, top and bottom surfaces of the model need to

be fixed. The relevant parameters of the surrounding rock are shown in Table 2, and the numerical simulation results are shown in Figure 5.

Figure 5 shows that when the reserved deformation m is small, there will be a prominent “ear shape” on the tunnel side wall, indicating that the displacement of the surrounding rock of the side wall will be slightly greater than the displacement at the vault and arch bottom. As the reserved deformation m increases, the displacement u_0 of the surrounding rock at the side wall, vault and arch bottom positions gradually increases, but the “ear shaped” phenomenon gradually disappears, and the displacement near the tunnel wall appears approximately circular. This is the same trend as in equation (51), where the displacement of the surrounding rock increases with an increase in the reserved deformation.

Extract the data on the maximum displacement of the surrounding rock at the tunnel wall in numerical simulation, draw a curve graph, and compare it with the relevant data of the analytical solution, as shown in Figure 6. From Figure 6, it can be seen that the variation law of the numerical and analytical solutions for the displacement of the surrounding rock is basically the same, both gradually increasing with the increase in the reserved deformation m . However, there is a certain distance between the two curves of the analytical and numerical solutions, indicating a certain degree of error between the analytical and numerical solutions.

The values of surrounding rock displacement was list in Table 3, which obtained by analytical and numerical methods under different reserved deformation and compare them. The comparison results are shown in Table 3.

Table 2. Relevant parameters of numerical simulation

Tunnel radius a/m	Elastic modulus E/GPa	Vertical pressure P_v/MPa	Cohesion C/MPa	Internal friction angle $\phi/^\circ$	Poisson's ratio μ	Lateral pressure coefficient λ
4	1	20	0.1	35	0.35	1.5

Table 3. Comparisons between analytical solutions and numerical simulation results of displacement of the surrounding rock

Displacement of surrounding rock/mm	Reserved deformation/mm					
	0	100	200	300	400	500
Analytical solution	291.22	298.50	305.78	313.07	320.35	327.63
Numerical solution	327.00	332.00	339.00	349.00	362.00	370.00
Error /%	10.94	10.09	9.80	10.30	11.51	11.45

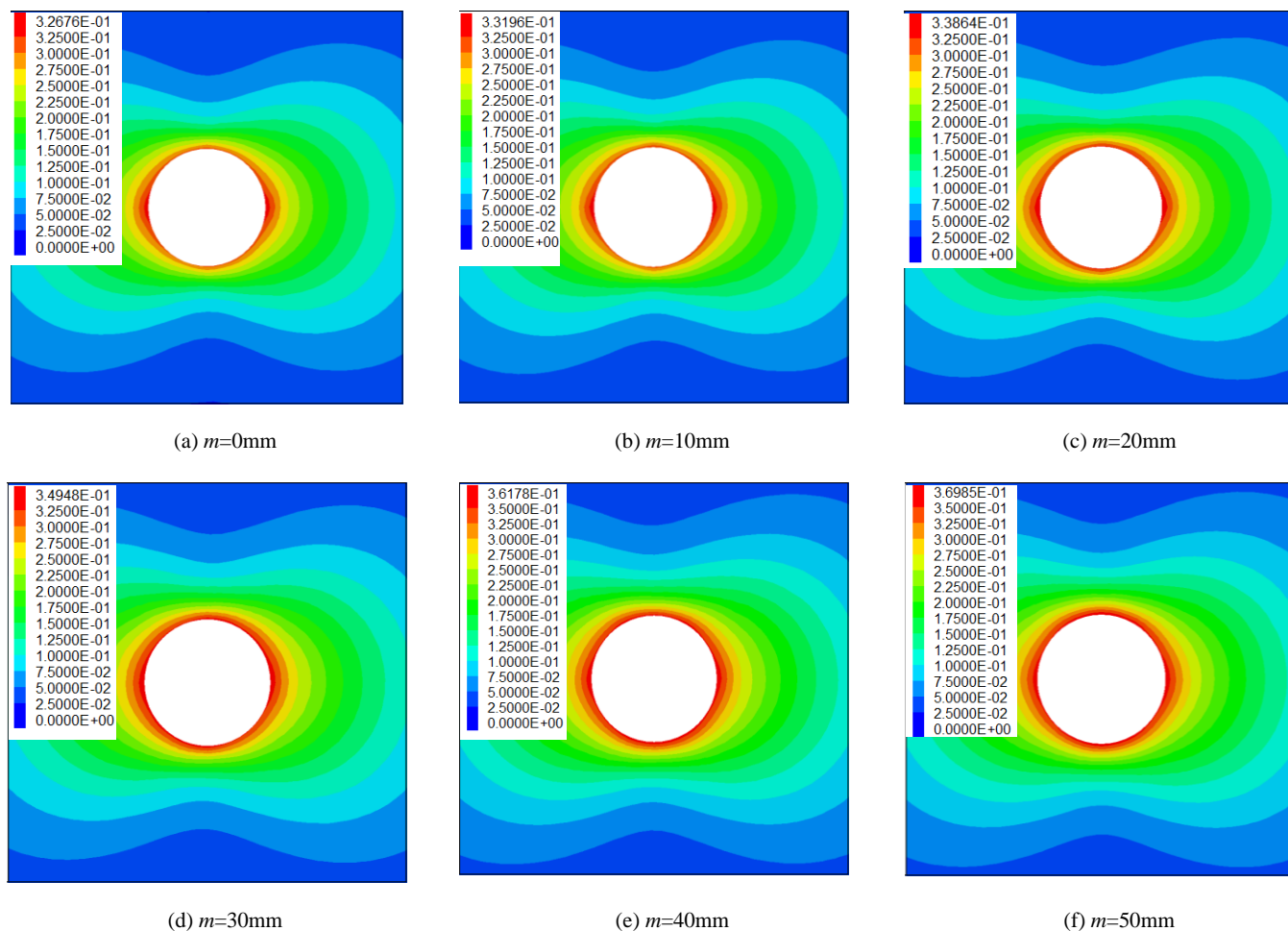


Fig. 5. Displacement nephograms of surrounding rock with different reserved deformations(m)

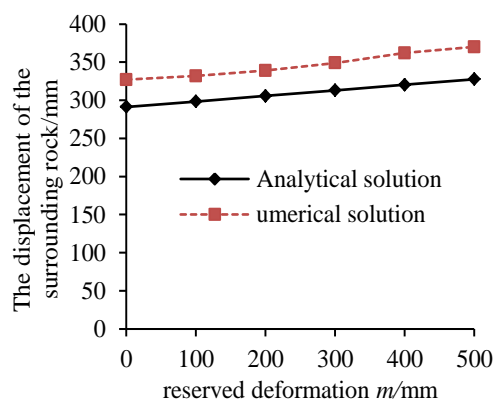


Fig. 6. Trend diagram of surrounding rock displacement with reserved deformation

5.2. Comparison and analysis of numerical solutions and analytical solutions for optimal reserved deformation

During the process of numerical simulation of the expression of the optimal reserved deformation, the reserved deformation m_0 needs to be solved by equation (23) when the support resistance p_i is known. Then the model is built according to the reserved deformation. When the

displacement of the surrounding rock is compared with the reserved deformation m_0 by numerical simulation, If the ratio of the displacement of the surrounding rock to the reserved deformation m_0 is close 1, it mean that equation (23) has high accuracy.

The constitutive model for numerical simulation uses the elastic-plastic model, and the basic parameters of the surrounding rock are listed in Table 1. The value of support resistance p_i is proposed to be 1, 2, 3, 4, 5 and 6 MPa. Based on the parameters of the surrounding rock in Table 1 and the values of support resistance p_i , the reserved deformation m_0 under different support resistance p_i can be obtained (as shown in Table 4) by substituting them into equation (23).

The modelling is based on the reserved deformation m_0 obtained from Table 4, and the numerical simulation results are shown in Figure 7.

Table 4. Analytical solution value of reserved deformation under different support resistances

Support resistance p_i /MPa	1	2	3	4	5	6
Reserved deformation m_0 /mm	349.4	238.8	190.1	162.1	143	129.0

From Figure 7, it can be seen that when the support resistance p_i is small, the displacement at the vault, side wall, and arch bottom is basically the same. As the support resistance p_i gradually increases, an “ear shaped” phenomenon appears at the side wall, indicating that the displacement of the surrounding rock at the side wall will be greater than the vault and arch bottom. The larger the support resistance p_i , the more obvious the “ear

shaped” phenomenon. However, when the support resistance p_i increases, the displacement of the surrounding rock at the vault, side walls, and arch bottom of the tunnel gradually decreases, which is consistent with the trend of the reserved deformation obtained from equation (23), which gradually decreases with the increase of the support resistance p_i .

Extract the displacement data of the surrounding rock from the numerical simulation and draw a curve graph, as shown in Figure 8.

From Figure 8, it can be seen that the reserved deformation m_0 solved by the analytical solution and the displacement u_0 of the surrounding rock obtained by numerical simulation gradually decrease with the increase of support resistance p_i , and the slope of the curve decreases. The two curves

of the analytical and numerical solutions do not coincide, indicating a certain degree of error between the analytical and numerical solutions.

At different support resistances, the values of reserved deformation obtained by solving equation (23) and the values of surrounding rock displacement obtained by numerical simulation were listed and compared. The comparison results are shown in Table 5.

From Table 5, it can be seen that as the with support resistance p_i gradually increases, the error is gradually increases. The maximum error is 11.61%. However, the error is basically within the range of 12%, indicating that equation (23) has a high degree of consistency between the analytical and numerical solutions.

Table 5. Comparison of reserved deformation and surrounding rock displacement

Support resistance p_i /MPa	1	2	3	4	5	6
Reserved deformation (analytical solution) /mm	349.41	238.82	190.45	162.08	142.98	129.05
Displacement of surrounding rock (numerical solution)/mm	384.00	264.00	212.00	181.00	161.00	146.00
Error /%	9.01	9.54	10.16	10.45	11.19	11.61

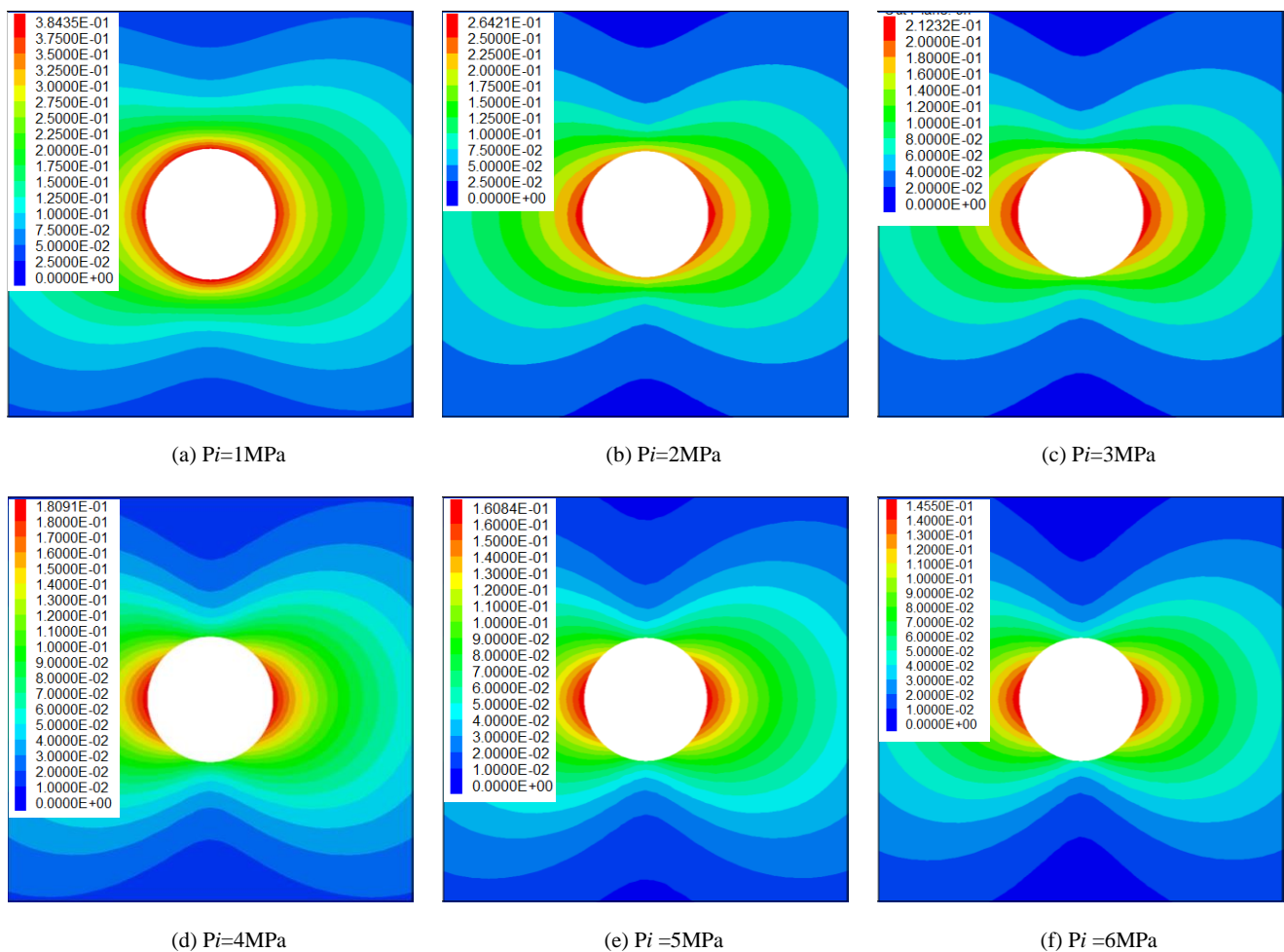


Fig. 7. Displacement nephogram of surrounding rock under different support resistances (m)

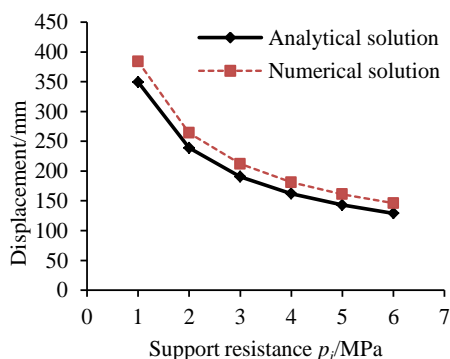


Fig. 8. Change trend diagram of surrounding rock displacement with support resistance

Although this article has derived an elastic–plastic expression for a circular cavity considering reserved deformation under non-axisymmetric load conditions, there are shortcomings in the research. First, the support of soft rock is timely and close to the tunnel face [51,52]. Therefore, it is necessary to consider the influence of the tunnel face. However, this article only deduces and analyses the analytical solution for the plane strain problem. Second, soft rock has creep properties [53,54], but this article ignores these properties and directly derives the elastic–plastic relationship. Obviously, there is a certain error in the actual situation, which can be seen in the numerical simulation. Finally, during the solution process, this article assumes that support resistance is constant, but in fact, support resistance will change with time [55]. Moreover, this article only considers the support resistance of the initial support and ignores the influence of the secondary lining. Therefore, in the subsequent research, the support effect of the tunnel face and secondary lining, the influence of time on the

displacement of surrounding rock and the variation of support resistance with time need to be considered.

6. Conclusion

On the basis of classical elastic–plastic theory, this article made some assumptions and derived the relevant expression equations for considering the reserved deformation under non-axisymmetric load conditions. The main conclusions are as follows:

(1) On the basis of classical elastic–plastic theory, the displacement expression of the surrounding rock is derived, considering the reserved deformation m_0 and the optimal reserved deformation m_0 under non-axisymmetric load conditions. The expression of support resistance with surrounding rock, support materials and crustal stress is derived on the basis of the known reserved deformation m .

(2) Through the method of controlling variables, the influencing factors of the reserved deformation are analysed. The analysis results show that the more the vertical pressure P_v , tunnel radius a and lateral pressure coefficient λ , the larger the optimal reserved deformation. However, with the increase of support resistance p_i , elastic modulus E , internal friction angle φ and cohesion C , the optimal reserved deformation becomes smaller.

(3) Numerical simulations were conducted using FLAC 3D software to calculate the displacement expression of the surrounding rock, considering the reserved deformation m and the expression of the optimal reserved deformation m_0 . The numerical simulation results were compared and analysed with the analytical solution results. The results show that the error between the numerical simulation and analytical solutions of the surrounding rock displacement expression, considering the reserved deformation m and the optimal reserved deformation m_0 , is within 12%, indicating that the numerical and analytical solutions of the two expressions have good consistency.

(4) In practical engineering, by inputting relevant parameters into the expression of the optimal reserved deformation, the value of the optimal reserved deformation can be obtained. So the expression of the optimal reserved deformation can providing a theoretical basis for determining the reserved deformation in practical engineering.

Acknowledgments

No funding was received to assist with the preparation of this manuscript.

Conflicts of Interest

All the authors claim that the manuscript is completely original. The authors also declare no conflict of interest.

Data availability

All relevant data related to this manuscript are available and can be provided upon reasonable request.

References

- Li JQ, Wang ZF, Wang YQ, Chang HT. Analysis and countermeasures of large deformation of deep-buried tunnel excavated in layered rock strata: A case study. *Engineering Failure Analysis*. 2023; 146: 107057. <https://doi.org/10.1016/j.engfailanal.2023.107057>
- Zhu QW, Li TC, Du YT, Zhang H, Ran JL, Li WT, Zhang SL. Failure and stability analysis of deep soft rock roadways based on true triaxial geomechanical model tests. *Engineering Failure Analysis*. 2022; 137: 106255. <https://doi.org/10.1016/j.engfailanal.2022.106255>
- Li N, Liu NF, Li GF. New method for stability evaluation of soil and soft rock tunnels. *Chinese Journal of Rock Mechanics and Engineering*. 2014; 33(09): 1812–1821. <https://doi.org/10.13722/j.cnki.jrme.2014.09.011>
- Sun XM, WC Zhao, Shen FX, Zhang Y, Jiang M. Study on failure mechanism of deep soft rock roadway and high prestress compensation support countermeasures. *Engineering Failure Analysis*. 2023; 143: 106857. <https://doi.org/10.1016/j.engfailanal.2022.106857>
- Li XF, Cheng GH, Li XQ, Zhang RH. A Study of Soft Rock Roadway Coupling Support in Xiajing Coal Mine. *Procedia Engineering*. 2014; 84: 812–817. <https://doi.org/10.1016/j.proeng.2014.10.500>
- Lin HF, Zhang BA. Study of Soft Rock Roadway Support Technique. *Procedia Engineering*. 2011; 26: 321–326. <https://doi.org/10.1016/j.proeng.2011.11.2174>
- He MC, Sui QR, Li MN, Wang ZJ, Tao ZG. Compensation excavation method control for large deformation disaster of mountain soft rock tunnel. *International Journal of Mining Science and Technology*. 2022; 32 (5): 951–963. <https://doi.org/10.1016/j.ijmst.2022.08.004>
- He MC. Latest progress of soft rock mechanics and engineering in China. *Journal of Rock Mechanics and Geotechnical Engineering*. 2014; 6(3): 165–179. <https://doi.org/10.1016/j.jrmge.2014.04.005>
- Liu Q, Li R, Tian W, Wang Y, Li X. Monitoring and support optimization analysis of surrounding rock pressure and initial supporting stress in deep-buried soft rock tunnel. *Revista Internacional de Métodos Numéricos para Cálculo y Diseño en Ingeniería*. 2021; 33 (2). <https://doi.org/10.23967/j.rimni.2021.01.0.03>
- Bizjak KF, Petkovsek B. Displacement analysis of tunnel support in soft rock around a shallow highway tunnel at Golovec. *Engineering Geology*. 2004; 75(1): 89–106. <https://doi.org/10.1016/j.enggeo.2004.05.003>
- Wang Q, Jiang B, Pan R, Li SC, He MC, Sun HB, Qin Q, Yu HC, Luan YC. Failure mechanism of surrounding rock with high stress and confined concrete support system. *International Journal of Rock Mechanics and Mining Sciences*. 2018; 102: 89–100. <https://doi.org/10.1016/j.ijrmms.2018.01.020>
- Meng FZ, Wong LNY, Zhou H, Wang ZQ, Zhang LM. Asperity degradation characteristics of soft rock-like fractures under shearing based on acoustic emission monitoring. *Engineering Geology*. 2020; 266: 105392. <https://doi.org/10.1016/j.enggeo.2019.105392>
- Meguid MA, Saada O, Nunes MA, Mattar J. Physical modeling of tunnels in soft ground: A review. *Tunnelling and Underground Space Technology*. 2008; 23(2): 185–198. <https://doi.org/10.1016/j.tust.2007.02.003>
- Zhang CL, Wiecek K, Xie ML. Swelling experiments on mudstones. *Journal of Rock Mechanics and Geotechnical Engineering*. 2010; 2(1): 44–51. <https://doi.org/10.3724/SP.J.1235.2010.00044>
- Zhu QW, Li TC, Zhang H, Ran JL, Li H, Du YT, Li WT. True 3D geomechanical model test for research on rheological deformation and failure characteristics of deep soft rock roadways. *Tunnelling and Underground Space Technology*. 2022; 128: 104653. <https://doi.org/10.1016/j.tust.2022.104653>
- Lin P, Liu HY, Zhou WY. Experimental study on failure behaviour of deep tunnels under high in-situ stresses. *Tunnelling and Underground Space Technology*. 2015; 46: 28–45. <https://doi.org/10.1016/j.tust.2014.10.009>
- Lai JX, Fan HB, Lai HP, Xie YL, Hu Z, Qiu JJ, Cao NQ. In-situ monitoring and analysis of tunnel deformation law in weak loess. *Rock and Soil Mechanics*. 2015; 36(7): 2003–2012+2020. <https://doi.org/10.16285/j.rsm.2015.07.023>
- Wang DY, Yuan JX, Zhu YQ, Liu J, Wang HF. Model test study of deformation characteristics and reasonable reserved deformation of shallow-buried loess tunnel with hard-flow plastic. *Rock and Soil Mechanics*. 2019; 40(10): 3813–3822. <https://doi.org/10.16285/j.rsm.2018.1308>
- Wang B, Yang Y, He C, Dai C, Zhou Y. Safety control criteria of displacement during construction of broken phyllite tunnels. *Chinese Journal of Rock Mechanics and Engineering*. 2016; 35 (11): 2287–2297. <https://doi.org/10.13722/j.cnki.jrme.2016.0353>
- Álvarez-Fernández MI, González-Nicieza C, Álvarez-Vigil AE, Herrera García G, Torno S. Numerical modelling and analysis of the influence of local variation in the thickness of a coal seam on surrounding stresses: Application to a practical case. *International Journal of Coal Geology*. 2009; 79(4): 157–166. <https://doi.org/10.1016/j.coal.2009.06.008>
- Barton N, Pandey SK. Numerical modelling of two stoping methods in two Indian mines using degradation of c and mobilization of φ based on Q-parameters. *International Journal of Rock Mechanics and Mining Sciences*. 2011; 48(7): 1095–1112. <https://doi.org/10.1016/j.ijrmms.2011.07.002>
- Muya M, H B, Wang JT, Li GC. Effects of Rock Bolting on Stress Distribution around Tunnel Using the Elastoplastic Model. *Journal of China University of Geosciences*. 2006; 17(4): 337–354. [https://doi.org/10.1016/S1002-0705\(07\)60008-9](https://doi.org/10.1016/S1002-0705(07)60008-9)
- Jia HS, Wang YW, Liu SW, Li YG, Shao RL, Wang GY, Guo ZQ, Wang L. Experimental study on double conical reamed anchorages for cable bolt boreholes in soft rock. *International Journal of Rock Mechanics and Mining Sciences*. 2022; 158: 105198. <https://doi.org/10.1016/j.ijrmms.2022.105198>
- Huang F, Zhu HH, Xu QW, Cai YC, Zhuang XY. The effect of weak interlayer on the failure pattern of rock mass around tunnel – Scaled model tests and numerical analysis. *Tunnelling and Underground Space Technology*. 2013; 35: 207–218. <https://doi.org/10.1016/j.tust.2012.06.01>
- Li YJ, Zhang DL, Fang Q, Yu QC, Xia L. A physical and numerical investigation of the failure mechanism of weak rocks surrounding tunnels. *Computers and Geotechnics*. 2014; 61: 292–307. <https://doi.org/10.1016/j.compgeo.2014.05.01>
- Cai WQ, Zhu HH, Liang WH, Wang XJ, Su CL, Wei XY. A post-peak dilatancy model for soft rock and its application in deep tunnel excavation. *Journal of Rock Mechanics and Geotechnical Engineering*. 2023; 15(3): 683–701. <https://doi.org/10.1016/j.jrmge.2022.05.014>
- Adachi T, Oka F. An elasto-plastic constitutive model for soft rock with strain softening. *International Journal for Numerical and Analytical Methods in Geomechanics*. 1996; 19(4): 233–247. <https://doi.org/10.1002/nag.1610190402>
- Alejano LR, Alonso E. Considerations of the dilatancy angle in rocks and rock masses. *International Journal of Rock Mechanics and Mining Sciences*. 2005; 42(4): 481–507. <https://doi.org/10.1016/j.ijrmms.2005.01.003>
- Walton G, Diederichs MS. A New Model for the Dilatation of Brittle Rocks Based on Laboratory Compression Test Data with Separate Treatment of Dilatancy Mobilization and Decay. *Geotechnical and Geological Engineering*. 2015; 33: 661–679. <https://doi.org/10.1007/s10706-015-9849-9>
- Rahjoo M, Eberhardt E. Development of a 3-D confinement-dependent dilatation model for brittle rocks; Part 1, derivation of a Cartesian plastic strain increments ratios approach for non-potential flow rules. *International Journal of Rock Mechanics and Mining Sciences*. 2021; 145: 104668. <https://doi.org/10.1016/j.ijrmms.2021.104668>
- Kargar AR. An analytical solution for circular tunnels excavated in rock masses exhibiting viscous elastic-plastic behavior. *International Journal of Rock Mechanics and Mining Sciences*. 2019; 124: 104128. <https://doi.org/10.1016/j.ijrmms.2019.104128>
- Zhao NN, Shao ZS, Yuan B, Chen XY, Wu K. Analytical approach to estimating the influence of friction slip contact between surrounding rock and concrete lining on mechanical response of deep rheological soft rock tunnels. *Applied*

- Mathematical Modelling. 2023; 113: 287-308. <https://doi.org/10.1016/j.apm.2022.09.012>
33. Ma ZL, Wang Y. Dynamic optimization of deformation allowance in large section loess tunnel. *Low Temperature Architecture Technology*. 2018, 40(12): 121-125, 137. <https://doi.org/10.13905/j.cnki.dwjz.2018.12.032>
 34. Yang WH. Research on reserved deformation of gently inclined soft rock highway tunnel. *Transpo World*. 2024; (Z1): 223-225. <https://doi.org/10.16248/j.cnki.11-3723/u.2024.z1.067>
 35. Yu WG, Zhu QW, Li LJ, Sun ZH. Research on reserved deformation of Baima Tunnel under different support parameters based on probability statistics. *Modern Tunnelling Technology*. 2021; 58(S1): 313-318. <https://doi.org/10.13807/j.cnki.mtt.2021.S1.039>
 36. Liu J, Liu YH, Wang T, Ma PG, Zhou HF. Prediction of Reserved Deformation in Loess Tunnel Based on Pearson Coefficient. *Journal of Anhui Jianzhu University*. 2024; 32(4): 64-70. <https://doi.org/10.11921/j.issn.2095-8382.20240410>
 37. Lee YK, Pietruszczak S. A new numerical procedure for elasto-plastic analysis of a circular opening excavated in a strain-softening rock mass. *Tunnelling and Underground Space Technology*. 2008; 23(5): 588-599. <https://doi.org/10.1016/j.tust.2007.11.002>
 38. Wu H, Fang Q, Zhang YD, Gong ZM. Zonal disintegration phenomenon in enclosing rock mass surrounding deep tunnels—Elasto-plastic analysis of stress field of enclosing rock mass. *Mining Science and Technology (China)*. 2009; 19(1): 84-90. [https://doi.org/10.1016/S1674-5264\(09\)60016-8](https://doi.org/10.1016/S1674-5264(09)60016-8)
 39. Ling CX. *Engineering Rock Mass Mechanics*. Harbin Institute of Technology Press, Harbin. 2020.
 40. Li L. Study on squeezing large deformation mechanism and control technology of phyllite tunnel. Dissertation, Beijing jiaotong University. 2017.
 41. Li WJ, Zhu YQ, et al. *Tunnel mechanics*. China Machine Press, Bei Jing. 2013.
 42. Zhang XD, Zhang SG, Jia BX. *Tunnel mechanics*. first ed, China University of Mining and Technology press, Xu Zhou. 2010.
 43. Li B, Yang X, Yuan Y, Liang YP, Li SQ, Zhu CQ, Peng WQ. Experimental research on the influence of different factors on the behaviour of broken coal and rock particles during compaction. *Construction and Building Materials*. 2023; 367: 130127. <https://doi.org/10.1016/j.conbuildmat.2022.130127>
 44. He JH, Li Y, Deng HC, Tang JM, Wang YY. Quantitative evaluation and influencing factors analysis of the brittleness of deep shale reservoir based on multiply rock mechanics experiments. *Journal of Natural Gas Geoscience*. 2022; 7(5): 295-307. <https://doi.org/10.1016/j.jnggs.2022.10.001>
 45. Gao Y, Xiao LZ, Wu BS. TSVD and Tikhonov methods and influence factor analysis for NMR data in shale rock. *Journal of Petroleum Science and Engineering*. 2020; 194: 107508. <https://doi.org/10.1016/j.petrol.2020.107508>
 46. Wang X, Cai M. FLAC/SPECFEM2D coupled numerical simulation of wavefields near excavation boundaries in underground mines. *Computers & Geosciences*. 2016; 96: 147-158. <https://doi.org/10.1016/j.cageo.2016.08.010>
 47. Caia M, Kaisera PK, Moriokab H, Minamib M, Maejimab T, Tasakac Y, Kurose H. FLAC/PFC coupled numerical simulation of AE in large-scale underground excavations. *International Journal of Rock Mechanics and Mining Sciences*. 2007; 44(4): 550-564. <https://doi.org/10.1016/j.ijmms.2006.09.013>
 48. Zapata VG, Jaramillo EB, Lopez AO. Implementation of a model of elastoviscoplastic consolidation behavior in Flac 3D. *Computers and Geotechnics*. 2018, 98: 132-143. <https://doi.org/10.1016/j.compgeo.2017.11.011>
 49. Ma YQ, Li Y, Gan Q, Zhi S. Numerical investigation of energy dissipation when shear wave passing through interface in rock mass. *Unconventional Resources*. 2023, 3: 142-154. <https://doi.org/10.1016/j.unres.2023.02.002>
 50. Yang KG, Gao DL. Numerical simulation of hydraulic fracturing process with consideration of fluid–solid interaction in shale rock. *Journal of Natural Gas Science and Engineering*. 2022; 102: 104580. <https://doi.org/10.1016/j.jngse.2022.104580>
 51. Panet M, Guenot A. Analysis of convergence behind the face of a tunnel. *International Journal of Rock Mechanics and Mining Sciences & Geomechanics Abstracts*. 1982; 20(1): 197-204. [https://doi.org/10.1016/0148-9062\(83\)91744-8](https://doi.org/10.1016/0148-9062(83)91744-8)
 52. Yu W, Wang B, Zi X, Guo XX, Wang ZY. Effect of prestressed anchorage system on mechanical behavior of squeezed soft rock in large-deformation tunnel. *Tunnelling and Underground Space Technology*. 2023; 131: 104782. <https://doi.org/10.1016/j.tust.2022.104782>
 53. Sun C.L, Li GC, Gomah ME, Xu JH, Sun YT. Creep characteristics of coal and rock investigated by nanoindentation. *International Journal of Mining Science and Technology*. 2020; 30 (6): 769-776. <https://doi.org/10.1016/j.ijmst.2020.08.001>
 54. Gutiérrez-Ch JG, Senen St, Zeng P, Jimenez R. DEM simulation of rock creep in tunnels using Rate Process Theory. *Computers and Geotechnics*. 2022; 142: 104559. <https://doi.org/10.1016/j.compgeo.2021.104559>
 55. Jia HL, Wang EY, Song XY, Zhang HJ, Li ZH. Correlation of electromagnetic radiation emitted from coal or rock to supporting resistance. *Mining Science and Technology (China)*. 2009; 19 (3): 317-320. [https://doi.org/10.1016/S1674-5264\(09\)60059-4](https://doi.org/10.1016/S1674-5264(09)60059-4)